RSC Advances

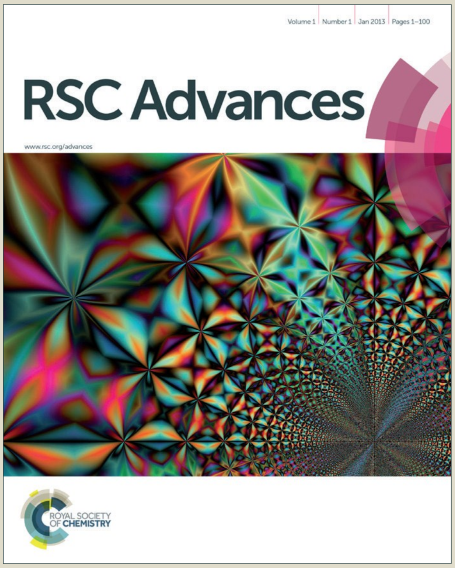
Volume 1 | Number 1 | Jan 2013 | Pages 1–100

RSC Advances

www.rsc.org/advances

ROYAL SOCIETY OF CHEMISTRY

ROYAL SOCIETY
OF CHEMISTRY

www.rsc.org/advances

RSC Advances

COMMUNICATION

Thermal and water dual-responsive shape memory poly(vinyl alcohol)/Al_2O_3 nanocomposite

Received 00th January 20xx,
Accepted 00th January 20xx

DOI: 10.1039/x0xx00000x

www.rsc.org/

Quanming Bai, Gongzheng Zhang, Bo Xu, Xianqi Feng, Haoyang Jiang, Huanjun Li*

We report on a new type of poly(vinyl alcohol) (PVA)/Al_2O_3 nanocomposite with fast thermal and water activated shape memory behavior via cyclic freezing/thawing method.

Shape memory polymers (SMPs) have attracted much attention for their capacity of recovering a permanent shape from a programmed temporary shape upon exposure to external stimuli such as heat, light, solvent, electric, and magnetic[1-8]. SMPs exhibit potential applications in smart biomedical devices, intelligent textile, implant devices for minimally invasive surgery, controlled drug release, aerospace fields and stimuli-responsive actuators [9-18] due to their high deformation strain, good processability and tunable transition temperatures. Despite of the promising application prospect of SMPs, their practical applications were severely limited by their weak mechanical properties compared with other shape-memory materials such as ceramics and metals.[19] Therefore, there is an urgent need to improve the mechanical properties of SMPs.

One of the approaches to overcome this shortcoming is to add nanofillers into polymer matrix to form polymer nanocomposites. Over decades, a variety of nanomaterials, including clay,[20] SiO_2,[21] cotton cellulose nanowhiskers (CNWs),[22] have been utilized to increase the mechanical strength of polymer-based materials. Also, numerous SMP nanocomposites were obtained by the same approach. For example, Pretsch and co-workers reported shape memory poly(ester urethane) (PEU) with various contents of thermochromic pigments (T-PIGs). These films exhibited the shape memory effect (SME) with the activation temperature. [23,24] Rana *et al*. prepared a kind of graphene/polyurethane block copolymers (PU) nanocomposite where the addition of graphene improved the mechanical properties and shape memory properties.[25] Amirian *et al*. explored poly(L-lactide-co-ε-caprolactone)/multiwalled carbon nanotubes (PLACL/MWCNTs) copolymer which could exhibits better SME and higher tensile strength.[26]

In contrast to the above mentioned polymers, PVA SMPs have drawn plenty of research interest in many fields,[27] due to their distinguished properties such as high hydrophilicity, nontoxicity, biocompatibility and better mechanical properties. Moreover, the hydroxyl groups in polymer backbone of PVA made it easier to be cross-linked and modified. Therefore, the fabrication of PVA nanocomposites with a range of inorganic nanofillers such as clay,[28] carbon nanotubes (CNTs)[29] and graphene oxide (GO)[30] have been widely investigated. On the other hand, nanosized Al_2O_3 is often selected as filler to improve mechanical properties of materials owing to its high strength and high hardness.[31] Group of Rao have reported the nanocomposites based on PVA and Al_2O_3/SiC nanowires. This work pointed out the strength of the composites increase with a small amount of nanowires.[32] In another study, Sonmez *et al*. prepared hybrid PVA/Al_2O_3 thin film with higher ultimate tensile strength.[33] These studies provide us the possibility to synthesis PVA SMPs with better mechanical performance. However, PVA/Al_2O_3 shape memory nanocomposites have not been reported.

So far, shape recovery can be induced by various external stimuli including temperature, light, electricity and magnetic fields. Among them, the most extensively studied stimulus was temperature which can be achieved either by direct or indirect heating induced by other stimuli such as microwave, light and electrical current. For example, Du *et al*. prepared chemical cross-linked PVA/glutaraldehyde SMP and found that samples with certain water content could be recovered rapidly under Microwave irradiation.[34] In another study, Zhang *et al*. first reported light polarization-controlled shape memory behaviour reinforced by gold nanorods (AuNRs) in PVA.[35] More recently, group of Lotfy also reported PVA-SMP cross-linked by ionizing radiation in the presence of carbon nanotubes that can display temperature-responsive shape memory behaviour.[36] However, from the biomedical applications point of view, it would be better to make use of water as the stimuli to trigger the shape memory of materials since it has no damage to tissue and interactive response to the blood when it was implanted into the human body. Moreover, the water induced shape recovery would be much easier and much applicable. Thus, water-induced SME has been extensively investigated in recent years.[37,38] Mendez *et al.*[22] exploited a series of water-activated

School of Chemical Engineering and Environment, Beijing Institute of Technology, Beijing 100081, China. E-mail: lihj@bit.edu.cn; zgongz99@bit.edu.cn

† Footnotes relating to the title and/or authors should appear here.
Electronic Supplementary Information (ESI) available: [details of any supplementary information available should be included here]. See DOI: 10.1039/x0xx00000x

shape memory materials by incorporating CNWs into the rubbery PU matrix. The water molecules regard as plasticizers when the water permeates into the polymer network. Recently, Qi *et al*. studied the PVA/GO nanocomposites, which have better shape memory properties induced by water.[39] Furthermore, although water can trigger shape recovery through the plasticizing effect due to the decrease of *T*g of PVA, thermal and water dual-responsive PVA SMPs have rarely been studied in previous shape memory nanocomposites.

Herein, we report on a new type of thermal and water dual-responsive shape memory PVA/Al_2O_3 nanocomposite via cyclic freezing/thawing method. Al_2O_3 nanoparticles (NPs) were chosen because of large amounts of hydroxyl groups on the surface of the NPs from high aqueous soluble alumina sols (ca. 17 wt%), enabling the facile physical crosslinking with PVA through hydrogen bond interaction, which is highly efficient route to improve the mechanical properties and exhibit a better shape memory behavior for PVA/Al_2O_3 nanocomposite. To the best of our knowledge, this is the first report about the shape memory of the PVA/Al_2O_3 nanocomposites. The advantages of the nanocomposite, including good hydrophilicity from PVA and aqueous soluble Al_2O_3 NPs components, biocompatibility, and dual-responsive shape memory, make it feasible for potential applications in many fields.

Scheme 1 illustrates the fabrication process and proposed formation mechanism of PVA/Al_2O_3 nanocomposite (PVA-A).[40, 41] Firstly, a certain amount of Al_2O_3 NPs dispersion was poured into PVA solution under constant stirring at 95 °C for 3 h. The prepared solutions were poured into a petri dish for cooling overnight. Secondly, the aqueous solutions were injected between two PTFE slides with 1.8 mm thick spacers. The samples were then subjected to one to five cycles of freezing for 24 h at -20 °C and thawing for 3 h at 25 °C. Then it was dried for 72 h at room temperature (25 °C) in air with the humidity at 40% to obtain the PVA/Al_2O_3 nanocomposites. The nanocomposite films consist of 5 wt% Al_2O_3 and 10 wt% Al_2O_3, hence forth mentioned as PVA-A5, and PVA-A10, were prepared respectively. During fabrication of the PVA/Al_2O_3 · films, the cross-linkages in the PVA-A was probably attributed to hydrogen bonds between the hydroxyl groups on Al_2O_3 NPs and the hydroxyl groups on polymer chains.[42] The adjacent PVA chains form crystallites in composite which was demonstrated by XRD at about 2θ=19.4°[43] (Fig.S2a). We also studied the influence of the freezing/thawing cycle number on crystalline behaviour as shown in Fig.S2b. It is worth noting that the degree of crystallinity increases with increasing the freezing/thawing cycle number. [44] The cyclic freezing/thawing causes an increase in PVA crystallinity, and the newly fabricated crystallites serve as additional physically crosslinking points, thus form a more densely three dimensional network. Therefore, the materials composed the hydrogen bonds network and PVA elastic network which result in the higher strength and be considered as fixed phase, while the reversible phase is amorphous phase. Unless otherwise stated, the specimen under investigation was undergone 3 cycles of freezing/thawing.

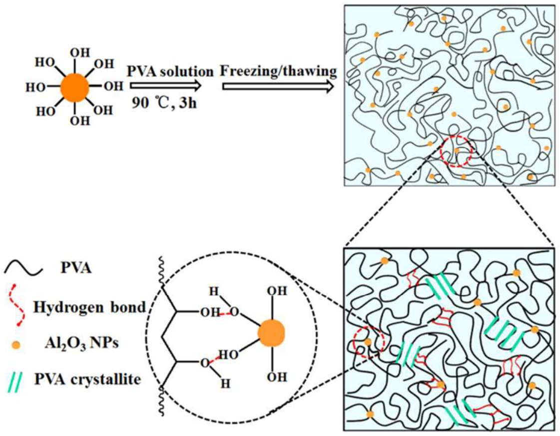

Scheme1. The fabricated process and formation mechanism of the PVA-A is illustrated. The red dash line represents the hydrogen bonds. The Al_2O_3 NPs were regard as sphere so as to simplify the drawing. The transmission electron microscope (TEM) image of Al_2O_3 NPs is shown in Fig.S1.

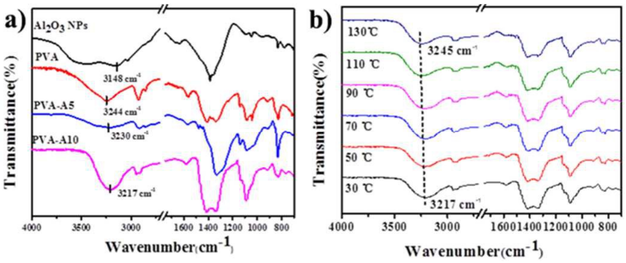

Fig.1 a) FTIR spectra of Al_2O_3 NPs, pure PVA and PVA/Al_2O_3 nanocomposites with different Al_2O_3 contents and b) differential spectra of the PVA-A10 film in the range of 700–4000 cm^{-1} at temperature of 30–130 °C.

Possible interactions between Al_2O_3 NPs and PVA chains were further explained by analysing the FT-IR spectra and temperature-variable FT-IR spectra. As shown in Fig.1a, the broad and strong absorption at 3000-3600 cm^{-1} is contributed to the symmetrical stretching vibration of O–H from the inter/intramolecular hydrogen bonds, which is located at the peak of 3244 cm^{-1}. The peaks at 2855 cm^{-1} and 2924 cm^{-1} are attributed to C-H stretching vibration from the PVA chains and the deformation vibration of CH2 groups appear at 1410 cm^{-1} and 1309 cm^{-1}. It is shown that symmetric C-C stretching vibrations is seen in 1140 cm^{-1}, indicating that the presence of crystalline region in PVA.[45] The sharp band at 1085 cm^{-1} is assigned to the C-O-C stretching vibration of acetyl group in polymer backbone. In case of PVA-A5 and PVA-A10 films, the symmetrical stretching vibration of hydroxyl group at 3244 cm^{-1} shift to 3230 cm^{-1} and 3217 cm^{-1} respectively, which indicated that there are strong hydrogen bond interactions between PVA chains and hydroxyl groups on Al_2O_3 NPs. Thus, these hydrogen bond interactions may be ascribed to the crosslinking of nanocomposite when Al_2O_3 NPs were uniformly dispersed in the PVA matrix. To further confirm and understand the hydrogen bonding between the PVA and Al_2O_3 NPs, we studied the temperature-variable FTIR spectra for PVA-10A film, as shown in Fig. 1b. With increasing temperature, the –OH stretching band shifts to large wavenumbers from 3217cm^{-1} to 3245 cm^{-1}, which indicates the broken of the weak hydrogen bonds.[46] The existence of weak hydrogen bond interactions between the ploymer and Al_2O_3 NPs could improve shape memory properties due to its reversible characteristic.

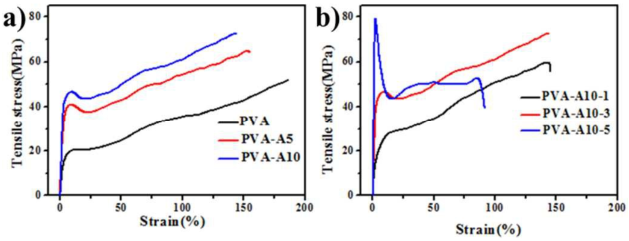

Fig.2 Typical stress–strain curves for PVA-A nanocomposite films with a) different Al_2O_3 content by three freezing/thawing cycles and b) different number of freezing/thawing cycles of PVA-A10.

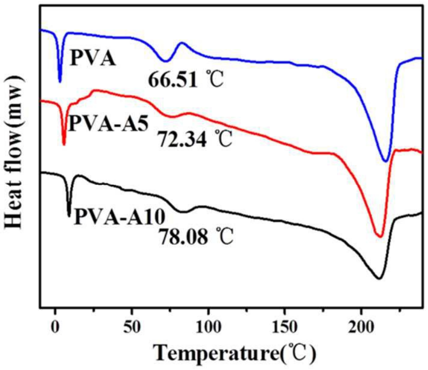

Fig.3 DSC thermograms of PVA-A nanocomposites with different alumina contents. Curve is presented in the range from -10 °C to 240 °C with heating rate 10 °C min^{-1}.

As a result of the uniform dispersion of Al_2O_3 NPs and the crosslinking (hydrogen bond interactions) structures, the nanocomposites exhibited good mechanical properties, such as higher ultimate stresses and large elongations at break. As shown in Fig.2, the stress-strain curves of PVA-A with various Al_2O_3 content and different times of freezing/thawing cycles are presented. It is obvious that the strength and elongation at break increases with increasing Al_2O_3 contents due to the formation of additional cross-linkages by introduction of Al_2O_3 NPs in the PVA matrix. The nanocomposites could be stretched to 140–190% (ε_b: elongation at break), and the tensile strength (σ) increased with Al_2O_3 content e.g., 51.9 MPa (pure PVA) and 72.3 MPa (PVA-A10). This indicates that the strong hydrogen bondings between the PVA chains and Al_2O_3 NPs are served as the physical cross-linkages for the nanocomposite. We also investigate the effect of the times of freezing/thawing cycles on the mechanical performance of nanocomposites. As display in Fig.2b, the ultimate stress of samples increases with increasing the times of freezing/thawing cycles. σ (ε_b) was 51.9 MPa (145%), 72.3 MPa (144%), and 79.2 MPa (92%) for PVA-A10 treated with 1, 3 and 5 freezing/thawing cycles, respectively. These results originate from the increase of the cross-linking density, which was confirmed by the decrease of swelling ratio for PVA-A10 sample in Fig.S3.[47] Furthermore, the elastic modulus significantly increases with increasing times of freezing/thawing cycles. For example, the elastic moduli of samples are 399 MPa, 876 MPa and 1274 MPa that correspond with 1, 3, and 5 freezing/thawing cycles respectively. Compared with the other PVA-SMP,[30] the mechanical properties of PVA-A is greatly improved.

The glass transition temperatures (*Tg*) of the PVA-SMPs and pure PVA were analyzed using differential scanning calorimetry (DSC) with the second heating thermograms (Fig.3a). The *Tg* of PVA is reported at around 86 °C, but observed at about 48 °C under humid conditions.[48] With increasing the content of Al_2O_3 in the PVA matrix, the *Tg* increased (*Tg* = 66.51 °C for PVA, *Tg* = 72.34 °C for PVA-A5 and *Tg* = 78.08 °C for PVA-A10). It is well known that the *Tg* is influenced by moisture, chain rigidity, molecular packing and linearity. The increasing of *Tg* may result from the interaction between the Al_2O_3 NPs and PVA, which limited the mobility of chains. The clear increasing in *Tg* of the PVA nanocomposite is very similar to the results reported in literature.[45] It can be observed from the figure that the melting temperature (*Tm*) is strongly influenced by the Al_2O_3 contents. With increasing of Al_2O_3 contents, the peaks of melting endotherm broaden and the *Tm* decreased, which could be associated with the decreasing of the crystallization. These results confirmed that the cross-linking between the PVA and Al_2O_3 NPs weakened the interaction among the polymer chains.[49]

On the basis of above discussion, we found that the hydrogen bonds formed between the polymer chains and the Al_2O_3 NPs, meanwhile it dissociated at a higher temperature, thus, we investigate the thermoresponsive shape recovery behaviours of the PVA and PVA-A10 nanocomposite (Fig.4). The rectangular strip samples were deformed to the circle shape above the *Tg* (90 °C), and the temperature was immediately cooled to room temperature (*T*<*Tg*) under constant stress to fix the temporary shape. Then, the deformed samples were placed on a platform at 90 °C. Surprisingly, it is recovered to the original shape quickly within 33 s. However, the pure PVA sample could not fully restore its initial shape within 90 s or even more than two hours. These results clearly show that PVA-A10 nanocomposite exhibits a better shape memory behaviour than pure PVA. This is attributed to the improved mechanical properties resulting from the incorporation of Al_2O_3 NPs as cross-linking points.[50]

We also investigated the relationship between the freezing/thawing cycle number and shape memory effect as shown in Fig.S4. The shape recovery was more quickly with increasing the number of freezing/thawing cycles. This may be resulted from the

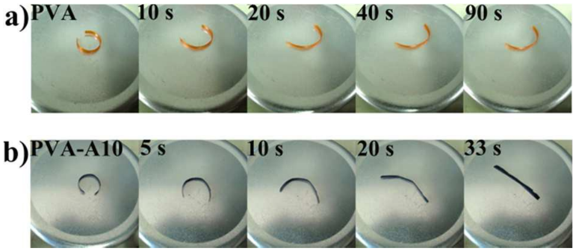

Fig.4 The macroscopic shape recovery of PVA-SMP performed at 90 °C. The pristine PVA and PVA-A10 strip was coated with red and blue dyestuff for easy observation. Permanent shape is straight shape.

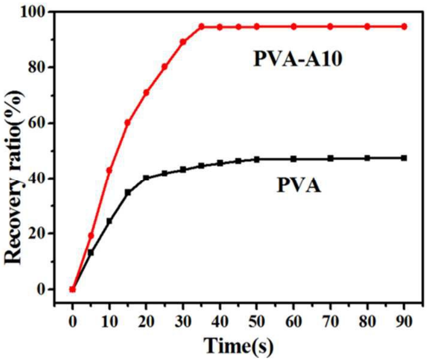

Fig.5 Shape memory recovery ratio of PVA and PVA-A10 at 90 °C.

increasing of crystallinity and decreasing of amorphous phase. Moreover, the temperature induced SME of the nanocomposite was quantified on the basis of report by Lendlein.[51] As shown in Fig.5, the shape fixity ratio (R_f) and shape recovery ratio (R_r) of the PVA, PVA-A10-1, PVA-A10-3 and PVA-A10-5 samples were studied in temperature-memory experiments. Compared with the pure PVA film, PVA-A10-3 and PVA-A10-5 recover to original shape quickly and the Rr can reach nearly 95%, though the R_f is lower than PVA. And the R_f and R_r of PVA and PVA-A10 with different freezing/thawing cycles are shown in Table S1. According to the experiments described above, we found that the PVA-A10 nanocomposite had the better thermoresponsive SME compared to pristine PVA film. Therefore, only the PVA-A10 nanocomposite was employed to study the water-responsive shape memory behaviour. The deformed specimen was immersed into water at room temperature and recorded with a digital camera. Similar to the thermoresponsive shape recovery behaviour, the PVA-A10 film has a better SME than the pristine PVA film. As shown in Fig.6, the pristine PVA film cannot be fully restored. In contrast, the PVA-A10 nanocomposite film quickly recovers to its original shape within 70 s. These results demonstrate that PVA-A10 shows a better shape memory behaviour than the pure PVA film. This clearly indicates that Al_2O_3 NPs can serve as additional physically cross-linking points and improve the tensile strength and modulus of the nanocomposite, which resulted in good water-induced SME. Moreover, the similar trend was observed for the dependence of water-induced shape memory effect on the freezing/thawing cycles (Fig.S5). Furthermore, it can be observed that the nanocomposite had an obvious increase in weight in the wake of shape recovery process (Fig.S3). This result was mainly attributed to the fact that the sample absorbed a certain amount of water. Therefore, this finding may support the previous statement that the SMP absorbed solvent molecules, and cause the decline of switching temperature and the interaction between the polymer chains.[37,38,52] The reason is that more free water molecule embedded into the PVA polymer matrix and the molecule acts as plasticizer, leading to the decrease of *Tg* and reducing the polymer stiffness,[31] and resulting in the shape recovery of PVA. When the switching temperature is lower than room temperature, soft segments begin to move, and then the shape recovery of PVA SMP occurred. The hydrogen bonding between PVA and Al_2O_3 was also influenced by water when the sample was immersed in it. Fig.S6 presents the FTIR spectra of PVA-10A with different immersion time. The peak of –OH shift from 3217 cm^{-1} to 3244 cm^{-1} which indicates the absorbed water forms hydrogen bonding with PVA, thus, the hydrogen bonding between PVA and Al_2O_3 nanocomposite weakened. We also investigated the thermal stability by TGA as shown in Fig.S7. The improved thermal stability may be supposed to result from interactions between Al_2O_3 NPs and PVA.

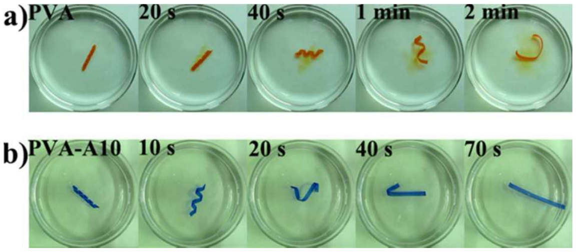

Fig.6 Shape memory effect of PVA and PVA-A10 samples (bent into spiral shape) in water. Permanent shape is straight shape.

In conclusion, we successfully prepared a novel dual-responsive shape-memory nanocomposite with PVA and Al_2O_3 NPs by cyclic freezing/thawing method. The physical cross-linking of 10 wt% Al_2O_3 NPs with PVA could significantly improve the mechanical properties of the nanocomposite. Simultaneously, the PVA-A10 nanocomposite exhibits an excellent thermally-induced and water-induced SME. Therefore, the multi-stimulus-responsive shape memory materials could be potentially applied in various fields such as biomedical and aerospace field.

Acknowledgements

This work was financially supported by the National Natural Science Foundation of China (21174017) and the Beijing Municipal Natural Science Foundation of China (2102040).

Notes and references

1. L. Sun, W. M. Huang, Z. Ding, Y. Zhao, C. C. Wang, H. Purnawali and C. Tang, *Mater. Des.*, 2012, **33**, 577–640.
2. T. Pretsch, *Polymers*, 2010, **2**, 120-158.
3. I. A. Rousseau, *Polym. Eng. Sci.*, 2008, **48**, 2075-2089.
4. R. Xiao, J. Guo and T. D. Nguyen, *RSC Adv.*, 2015, **5**, 416-423.
5. W. Wu, L. Yao, T. Yang, R. Yin, F. Li and Y. Yu, *J. Am. Chem. Soc.*, 2011, **133**, 15810-15813.
6. D. Quitmann, N. Gushterov, G. Sadowski, F. Katzenberg and J. C. Tiller, *ACS Appl. Mater. Inter.*, 2013, **5**, 3504-3507.
7. Y. Huang, J. Liang and Y. Chen, *J. Mater. Chem.*, 2012, **22**, 3671.
8. M. Y. Razzaq, M. Behl, K. Kratz and A. Lendlein, *Adv. Mater.*, 2013, **25**, 5730-5733.
9. W. M. Huang, B. Yang, Y. Zhao and Z. Ding, *J. Mater. Chem.*, 2010, **20**, 3367-3381.
10. F. Ji, Y. Zhu, J. Hu, Y. Liu, L. Y. Yeung and G. Ye, *Smart Mater Struct*, 2006, **15**, 1547-1554.
11. A. Lendlein and R. Langer, *Science*, 2002, **296**, 1673-1676.
12. Wache, H. M. Tartakowska, D. J. Hentrich, A. Wangner, M. H. *J. Mater. Sci*. 2003 , **14** , 109.
13. H. Lu, J. Gou, J. Leng and S. Du, *Appl. Phys. Lett.*, 2011, **98**, 1-13.
14. J. L. Hu, Y. Zhu, H. H. Huang and J. Lu, *Prog. Polym. Sci.*, 2012, **37**, 1720-1763.
15. M. Bothe and T. Pretsch, *Macro. Chem. Phys.*, 2012, **213**, 2378-2385.
16. T.-H. Kang, J.-M. Lee, W.-R. Yu, J. H. Youk and H. W. Ryu, *Smart. Mater. Struct.*, 2012, **21**, 035028.
17. S. Imai and K. Sakurai, *Precision Eng*, 2013, **37**, 572-579.
18. M. Bothe and T. Pretsch, *J. Mater. Chem. A.*, 2013, **1**, 14491-14497.
19. M. L. Auad, V. S. Contos, S. Nutt, M. I. Aranguren and N. E. Marcovich, *Polym Int*, 2008, **57**, 651-659.
20. S. Rezanejad and M. Kokabi, *Eur. Polym. J.*, 2007, **43**, 2856-2865.
21. C. Y. Bae, J. H. Park, E. Y. Kim, Y. S. Kang and B. K. Kim, *J. Mater. Chem.*, 2011, **21**, 11288-11295.
22. J. Mendez, P. K. Annamalai, S. J. Eichhorn, R. Rusli, S. J. Rowan, E. J. Foster and C. Weder, *Macromolecules*, 2011, **44**, 6827-6835.
23. M. Ecker and T. Pretsch, *RSC Adv*, 2014, **4**, 46680-46688.
24. M. Ecker and T. Pretsch, *RSC Adv*, 2014, **4**, 286-292.
25. S. Rana, J. W. Cho and L. P. Tan, *RSC Adv*, 2013, **3**, 13796-13803.
26. M. Amirian, A. N. Chakoli, J. Sui and W. Cai, *J Polym Res*, 2012, **19**, 9777.
27. C. M. Hassan and N. A. Peppas, *Macromolecules*, 2000, **33**, 2472-2479.
28. Y. H. Yu, C. Y. Lin, J. M. Yeh and W. H. Lin, *Polymer*, 2003, **44**, 3553-3560.
29. P. Miaudet, A. Derre, M. Maugey, C. Zakri, P. M. Piccione, R. Inoubli and P. Poulin, *Science*, **318**, 1294-1296.
30. H. K. F. Cheng, N. G. Sahoo, Y. P. Tan, Y. Pan, H. Bao, L. Li, S. H. Chan and J. Zhao, *ACS Appl. Mater. Inter.*, 2012, **4**, 2387-2394.
31. M. Wisniewska, S. Chibowski, T. Urban and D. Sternik, *J Therm Anal Calorim*, 2011, **103**, 329-337.
32. S. R. C. Vivekchand, U. Ramamurty and C. N. R. Rao, *Nanotechnology*, 2006, **17**, S344-S350.
33. M. Sonmez, D. Ficai, A. Stan, C. Bleotu, L. Matei, A. Ficai and E. Andronescu, *Mater Lett*, 2012, **74**, 132-136.
34. H. Du, Y. Yu, G. Jiang, J. Zhang and J. Bao, *Macromol. Chem. Phys.*, 2011, **212**, 1460-1468.
35. H. Zhang, J. Zhang, X. Tong, D. Ma and Y. Zhao, *Macromol. Rapid Commun*, 2013, **34**, 1575-1579.
36. A. A. Basfar and S. Lotfy, *Radiat.Phys. Chem.*, 2015, **106**, 376-384.
37. W. M. Huang, B. Yang, L. An, C. Li and Y. S. Chan, *Appl. Phys. Lett.*, 2005, **86**, 114105.
38. Y. Zhu, J. L. Hu, H. S. Luo, R. J. Young, L. B. Deng, S. Zhang, Y. Fan and G. D. Ye, *Soft Matter*, 2012, **8** , 2509.
39. X. Qi, X. Yao, S. Deng, T. Zhou and Q. Fu, *J. Mater. Chem. A*, 2014, **2**, 2240-2249.
40. W. Yao, C. Geng, D. Han, F. Chen and Q. Fu, *RSC Adv.*, 2014, **4**, 39588.
41. J. Chengbin, Z. Xiujian, W. Xina, T. Haizheng and L. Aiyun, *Mater Lett*, 2005, **59**, 3742-3745.
42. S. Mallakpour and M. Dinari, *J Reinf Plast Comp*, 2013, **32**, 217-224.
43. S. Pandey, S. K. Pandey, V. Parashar, G. K. Mehrotra and A. C. Pandey, *J. Mater. Chem.*, 2011, **21**, 17154.
44. R. Ricciardi, F. Auriemma, C. De Rosa and F. Laupretre, *Macromolecules*, 2004, **37**, 1921-1927.
45. A. Singhal, M. Kaur, K. A. Dubey, Y. K. Bhardwaj, D. Jain, C. G. S. Pillai and A. K. Tyagi, *RSC Adv*, 2012, **2**, 7180.
46. S. Sugumaran, C. S. Bellan and M. Nadimuthu, *Iran. Polym. J.*, 2015, **24**, 63-74.
47. K. Haraguchi, H-J Li, L-Y Song and K. Murata, *Macromolecules* 2007, **40**, 6973-6980.
48. J. Lee, D. Bhattacharyya, A. J. Easteal and J. B. Metson, *Curr Appl Phys*, 2008, **8**, 42-47.
49. H. Javier Salavagione, G. Martinez and M. A. Gomez, *J. Mater. Chem.*, 2009, **19**, 5027-5032.
50. Kang, S. M, Kim, M. J, Kwon, S. H, Park, H, Jeong, H. M and Kim, B. K, *J. Mater. Res*., 2012, **27**, 2837-2843.
51. A. Lendlein and S. Kelch, *Angew. Chem., Int. Ed.*, 2002, **41**,2034
52. H. Du and J. Zhang, *Soft Matter*, 2010, **6**, 3370.